IEEE Access
Multidisciplinary | Rapid Review | Open Access Journal

Received April 18, 2019, accepted May 11, 2019, date of publication May 21, 2019, date of current version June 5, 2019.

Digital Object Identifier 10.1109/ACCESS.2019.2917892

Review on Photonic Crystal Fibers With Hybrid Guiding Mechanisms

DORA JUAN JUAN HU[1], (Senior Member, IEEE), ZHILIN XU[2], (Member, IEEE), AND PERRY PING SHUM[3,4], (Senior Member, IEEE)

[1]Institute for Infocomm Research, A*STAR, Singapore 138632
[2]MOE Key Laboratory of Fundamental Physical Quantities Measurement & Hubei Key Laboratory of Gravitation and Quantum Physics, PGMF and School of Physics, Huazhong University of Science and Technology, Wuhan 430074, China
[3]School of Electrical and Electronic Engineering, Nanyang Technological University, Singapore 639798
[4]CINTRA CNRS/NTU/THALES, UMI 3288, Singapore 639798

Corresponding author: Dora Juan Juan Hu (jjhu@i2r.a-star.edu.sg)

This work is supported by National Research Foundation Singapore (NRF) (NRF-CRP13-2014-05), the Fundamental Research Funds for the Central Universities (HUST: 2019kfyXJJS156), Open Fund of IPOC (Beijing University of Posts and Telecommunications), and Singapore Ministry of Education Academic Research Fund Tier 1 (RG89/16).

ABSTRACT Photonic crystal fibers (PCFs) with hybrid guiding mechanisms have undergone substantial development in recent years. Due to the co-existence of index-guiding and photonic bandgap (PBG)-guiding mechanisms in this special class of PCFs, many peculiar properties have been investigated and demonstrated as advantageous and favorable in many applications. This review paper provides a comprehensive review of the recent progress of these hybrid guiding PCFs. The first part explains the principles of the hybrid guiding mechanisms in the PCF structures. The hybrid guiding PCFs are realized in three approaches, including polarization-dependent hybrid guiding PCFs, radial hybrid guiding PCFs, and two-core hybrid guiding PCFs. This is followed by a review of various development and applications for each type of hybrid guiding PCFs in the second part, including tunable filters, high power lasers, nonlinear optics, and polarization optics and sensing applications. Finally, the considerations and challenges on the potential applications of the hybrid guiding PCFs are discussed.

INDEX TERMS Hybrid guiding PCFs, photonic crystal fibers (PCFs), polarization-dependent hybrid guiding PCFs, radial hybrid guiding PCFs, two-core hybrid guiding PCFs.

I. INTRODUCTION

Photonic crystal fibers (PCFs), a breakthrough invention of fiber optic technology which breaks the physical limits of conventional optical fibers and introduces new guiding mechanisms into the structure, have been rapidly developed with unparalleled features and performance for numerous applications in the past two decades. First of all, conventional optical fibers usually have a limited refractive index difference between the core and the cladding due to limited doping concentration which is associated with high attenuation loss. Secondly, small core size in conventional optical fibers to ensure single mode transmission often leads to undesirable nonlinearity effects for communication applications or hindrance effect on high power applications. In addition, there is not much flexibility to significantly enhance the nonlinear effects in conventional optical fibers for nonlinear optics applications. In comparison, PCFs with arrays of air holes in the cross sections over entire length of the fibers, allow large controllability and flexibility in tailoring the microstructure geometry, the air filling fraction, the materials to fill within the air holes for more versatile functionalities, and even hollow core guidance can be realized by new light guiding mechanisms. Since its discovery, PCFs have demonstrated many unique features and provided significant flexibilities in designing and controlling the optical properties that are not attainable in conventional optical fibers. The flourished research progress in the PCF technology was reviewed by numerous articles with various emphasis. For example, the pioneering works in PCFs were reviewed in [1]–[3]. PCFs for sensing applications were reviewed in [4]–[6]. In addition, the PCFs can be used as a substrate for inclusions of other materials, such as liquid, gas and solid for various applications as reviewed in [7]. The PCF-based

The associate editor coordinating the review of this manuscript and approving it for publication was San-Liang Lee.

optofluidic sensor applications was reviewed in [8]. It should be highlighted that PCFs are a desirable platform to integrate with plasmonic micro-nanostructures for greater opportunities in performance and versatility. The works on plasmonic PCFs and their applications were reviewed in [9]–[11]. The usage of PCFs in development of novel fiber lasers was reviewed in [12]. In addition, PCFs have introduced broad opportunities for nonlinear optics as reviewed in [13], [14]. As it is a rapidly developing field, active research effort is being continuously devoted to the advancement of the PCF technologies and realizations of the various applications.

PCFs can be characterized by various guiding mechanisms, including index-guiding mechanism, photonic bandgap (PBG)-guiding mechanism, inhibited coupling-guiding mechanism, antiresonance-guiding mechanism, and twist-induce guiding mechanism. The detailed explanation of each guiding mechanism in different types of PCFs was provided in a recent review article [7]. Different from most reported PCF structures, in which only one guiding mechanism is present, there is a special group of PCFs with co-existence of both index-guiding and PBG-guiding mechanism, referred as hybrid guiding PCFs in the subsequent sections in this article. The first experimental study of such hybrid guiding PCFs was reported in [15], followed by a theoretical study as reported in [16]. Because of the interactions between the two guiding mechanisms, hybrid guiding PCFs exhibit interesting properties which enable many exploitable applications. Therefore, they received significant attention from the PCF research community. Substantial development in hybrid guiding PCFs has been witnessed, from realizations of tunable filters, high power lasers, nonlinear optics, and polarizations optics to various sensing applications. To the best of our knowledge, there is none review paper on the hybrid guiding PCFs from the angle of the guiding mechanism. It is the focus and the purpose of this review article, to provide an in-depth and comprehensive review on the progress and the prospects of the hybrid guiding PCFs that can serve as a guide and a reference for interested researchers for further explorations and investigations. In this review, the operating principles of the hybrid guiding mechanisms in the hybrid guiding PCFs are introduced, followed by an overview on the progress in the various development and applications. Finally, a discussion on their opportunities and challenges is presented.

II. HYBRID GUIDING MECHANISMS IN PCFs

A. INDEX GUIDING MECHANISM

Similar to conventional optical fibers, the light guidance of the PCFs can be realized by trapping and propagating the light in the core region with higher refractive index than that of the cladding region. In conventional optical fibers, dopants are added to the core regin to obtain higher refractive index. In PCFs, the effective refractive index in the holey cladding region can be characterized by a parameter n_{fsm}

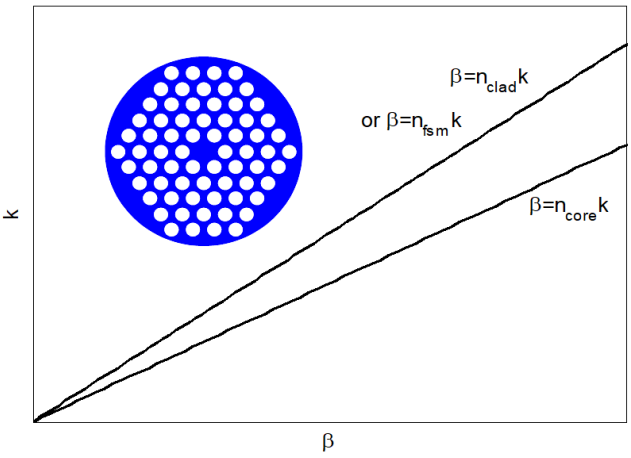

FIGURE 1. Dispersion curve for index-guiding mechanism in conventional optical fibers and solid core PCFs.

corresponding to the fundamental space filling mode of the assumed infinite periodic structure [17]. The value of n_{fsm} lies between the refractive index of air and silica, and can be flexibly controlled to realize very high index contrast or low index contrast by engineering the lattice geometry and air filling ratio of the holey structure. This flexibility has enabled PCFs to demonstrate many favorable features such as endless single mode operation [17], very large numerical aperture [18], large mode are with low bend loss [19], [20], high nonlinearities with dispersion tailoring [21], [22], single polarization single mode operation [23], [24], and high birefringence [25], [26] *etc.*

The index-guiding principle can be illustrated from the β-k plot where β is the propagation constant, and k is the free space wavenumber in **Fig. 1.** For a homogeneous and isotropic medium with refractive index n, the radiation line $\beta = nk$ defines the onset of the total internal reflection (TIR) for light that is incident from another medium with a higher refractive index. On the radiation line, the critical angle is reached. Above the radiation line, the light is free to propagate whereas the light is evanescent below the radiation line. In conventional optical fibers, the refractive indices in the core and the cladding are denoted as n_{core} and n_{clad} respectively. In index-guiding PCFs, the holey cladding's radiation line $\beta = n_{fsm}k$. The inset figure shows a typical solid core PCF with air holes arranged in triangular lattice embedded in silica. The core's radiation line lies below the cladding's radiation line in both conventional optical fibers and index-guiding PCFs due to higher refractive index in the core region. Therefore, optical confinement by index-guiding mechanism in the core region of an optical fiber (including both conventional optical fibers and index-guiding PCFs) only occurs in the region enclosed by the cladding's and core's radiation lines. Because of the similarity of the guiding mechanism in the index-guiding PCFs and that is present in the conventional optical fibers, index-guiding mechanism is also referred as modified total internal reflection (MTIR) guiding mechanism.

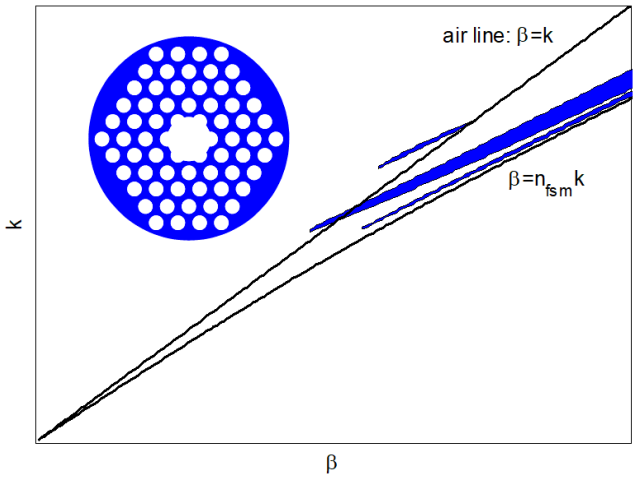

FIGURE 2. Dispersion curve for PBG-guiding in hollow core PCFs.

B. PBG-GUIDING MECHANISM

The shaded 'finger tips' regions in **Fig. 2** refer to bandgaps formed in a typical holey structure with triangular lattice configuration embedded in silica, where it is forbidden for propagating modes within the holey structure. The inset figure shows a hollow core PCF with holey structure in the cladding. The hollow core acts as a 'defect' in the photonic crystal structure. The radiation lines of the core and the cladding are denoted as $\beta = k$ and $\beta = n_{fsm}k$ respectively. As the refractive index of the hollow core is lower than n_{fsm}, the core's radiation line lies above the cladding's radiation line. It is clear that index-guiding mechanism does not allow optical confinement in the hollow core PCFs. Nevertheless, the bandgaps that exist above the core's radiation line can be utilized to realize hollow core guidance. The principle of PBG-guiding mechanism is therefore to utilize the bandgaps above the core's radiation line, i.e. the airline, within which the light is not allowed to propagate in the photonic crystal cladding but confined in the hollow core. The same principle can be applied to other PBG PCFs with low index core or all solid PBG fibers.

C. HYBRID GUIDING MECHANISM

It is possible to realize optical confinement by both index-guiding and PBG-guiding mechanisms in the same PCF, which are referred as hybrid guiding PCFs in the article. The co-existence of both guiding mechanisms has led to many interesting features that were later demonstrated by researchers as useful and desirable features in applications including filters, fiber lasers and amplifiers, nonlinear optics, polarization optics, and sensors.

There are three approaches of creating the co-existence of two guiding mechanisms in PCF structures. The first approach is to break the symmetry of the degenerated fundamental mode in the PCF structure and the two orthogonally polarized core modes are formed by different guiding mechanisms [15]. In this approach, high index materials such as high-index rods were replacing one or more rows of air holes

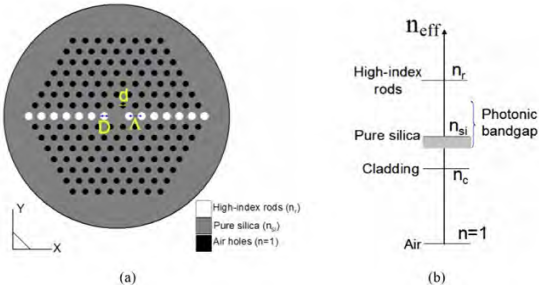

FIGURE 3. The concept of a hybrid PCF: (a) Schematic of the hybrid PCF, and (b) relevant effective indices. The regime where hybrid guidance is possible is shaded grey. (Reproduced with permission. [15] Copyright 2006, OSA).

in the holey cladding of a silica core PCF, so that light can be guided by index-guiding mechanism in one direction and by PBG-guiding mechanism in the other direction. One example of the reported hybrid guiding PCF structure is shown in **Fig. 3** [15]. B-doped and F-doped silica were introduced into all solid PCFs with Ge-doped cladding rods to form the hybrid guiding mechanism [27]. Similar structures were realized by selectively infiltrating high-index liquids into the air holes to create hybrid guiding mechanisms [28]. Using capillary effect, liquid can go up to ten centimeters or several tens of centimeters in micron air holes, depending on the liquid surface tension and liquid density. The liquid filled PCFs are commonly used for short length applications, e.g. in centimeter scale, where loss is not a significant concern.

Alternatively, the polarization-dependent guiding mechanism can be realized by making use of the birefringent properties of the infiltration material, i.e. nematic liquid crystal (NLC) within the holey cladding of PCFs. Sun *et al*. proposed a non-silica glass PCF structure infiltrated with NLC into the air holes [29]. The refractive index of the background glass, the ordinary and extraordinary refractive indices of the NLC, are n_b, n_o and n_e respectively, satisfying the condition: $n_e > n_b > n_o$. Using external electric filed control, the NLC molecules can be aligned along the direction of the electric field, e.g. along the y-direction as shown in **Fig. 4**. The proposed fiber thus relies on index-guiding mechanism along the x-direction, and bandgap-guiding mechanism along y-direction. It should be noted that if the fiber glass material has a refractive index that satisfies the condition: $n_e > n_o > n_b$, instead of hybrid guiding mechanisms, the liquid crystal filled PCF (LCPCF) would have polarization-dependent bandgap-guiding [30]. Both designs can be used to achieve ultrahigh birefringence, as well as single polarization single mode applications [29], [30].

The second approach is to construct radial hybrid guiding PCF structures in which the central core is surrounded by layers of photonic crystal cladding which support both the index-guiding and bandgap-guiding mechanisms. The coexistence of hybrid guiding mechanisms can be achieved by introducing index guidance in a bandgap guiding PCF with a photonic crystal cladding. The index guidance is achieved by either lowering the effective index of the cladding, or raising

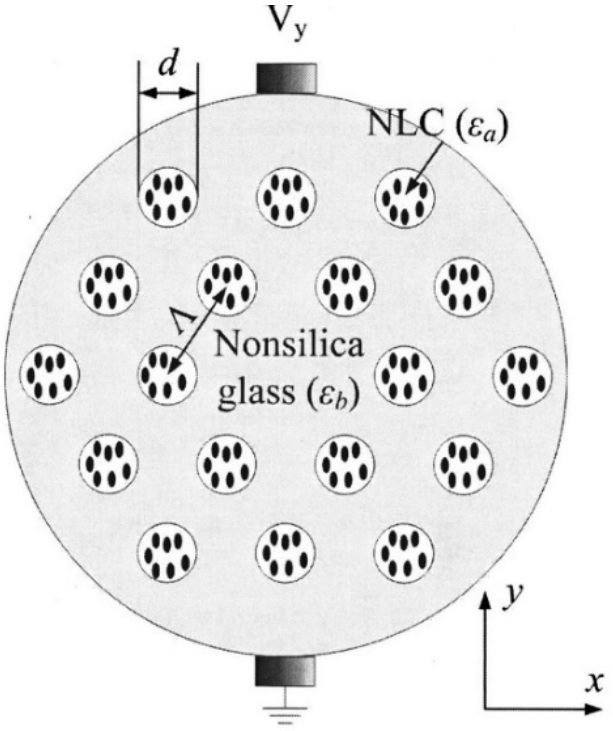

FIGURE 4. Schematic of the LCPCF with an optic axis of an NLC along the y direction. (Reproduced with permission. [29] Copyright 2007, OSA).

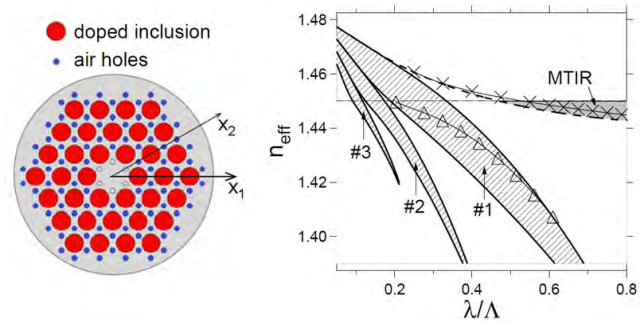

FIGURE 5. Schematic transversal cut and associated band diagram for the hybrid guiding PCF. The three first bandgaps are shaded in light gray. Also shown the fundamental space filling mode index (dashed line). The region where MTIR guidance is possible is shaded in dark gray. The effective index of the fundamental core mode in the 1st bandgap (triangle) and the fundamental MTIR guided core mode (cross) are also plotted. The material dispersion has not been considered here. (Reproduced with permission. [32] Copyright 2008, OSA).

the refractive index of the core [31]–[34]. For example, in the reported design of [32], as shown in **Fig. 5**, interstitial air holes are introduced into the all-solid bandgap PCF to reduce the effective index of the photonic crystal cladding n_{fsm} . The core region is formed by removing the first ring of air holes and can be considered as a defect in the photonic crystal lattice. As a result, the fiber structure supports both the index-guiding mechanism as the refractive index of the silica core is higher than n_{fsm} , and bandgap-guiding mechanism due to the photonic crystal cladding structure. The band and dispersion diagram of the hybrid fiber structure is also shown in **Fig. 5**, showing two fundamental modes guided by index-guiding

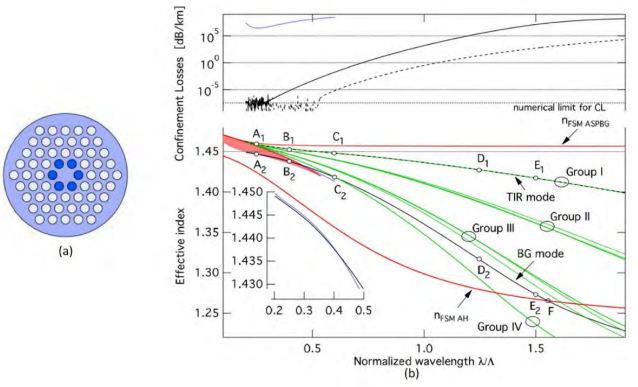

FIGURE 6. (a) Cross section of the radially hybrid fiber. Darker blue corresponds to higher refractive index. (b) Bottom: In black, effective indices of the BG-like mode (solid line) and MTIR-like mode (dashed line) of the fiber RH. Green lines correspond to the effective indices of the 12 cladding modes that can be associated to LP_{01} supermodes of the 6 high index rods. Red curves represent the effective index of the fundamental space filling mode calculated for an infinite structure with the periodicity of the Fiber ASPBG cladding (top curve) and with the periodicity of the Fiber 7D cladding (bottom curve). The dispersion curve of the Fiber ASPBG fundamental mode is plotted in blue in the first bandgap (red hatched area), the inset being a zoom to facilitate the comparison between this mode and the BG-like mode of the fiber RH. Top: Corresponding core modes confinement losses. (Reproduced with permission. [35] Copyright 2012, OSA).

and bandgap-guiding mechanism respectively. The proposed fiber design can be used to achieve phase matching between the two fundamental modes guided by different mechanisms, for second or third harmonic generation.

Alternatively, photonic bandgap guidance can be introduced to an index-guiding PCF to obtain hybrid guidance [35]–[37]. For example, a ring of high-index rods is introduced to surround the solid core in an index-guiding PCF as shown in **Fig. 6(a)**. The proposed PCF structure supports both a bandgap-like core mode and the index-guided core mode due to the coexistence of two guiding mechanisms. The bandgap-like core mode resembles the properties of the core mode of an all solid bandgap fiber with doped rods in the cladding. However, the bandgap-like core mode exhibits broader spectral range than the bandgap and significantly reduced confinement losses as compared to the all solid bandgap fiber. The numerical studies of the proposed fiber design are summarized in **Fig. 6(b)**, showing the effective index and the confinement loss of the bandgap-like core mode and index-guided core mode in the radially hybrid fiber. The proposed fiber design can be used as mode filter, or be used to ease phase matching conditions for nonlinear optics [35].

The third approach is to construct a two-core PCF structure with each core guiding light using either index-guiding or bandgap-guiding mechanism. For example, Sun proposed a two-core PCF coupler structure with one core surrounded six rods with higher refractive material and the other core surrounded by holey cladding as shown in **Fig. 7**. Compared to broadband fiber coupling structures, the phase matching in the proposed hybrid guiding fiber is satisfied at a particular wavelength between the two core modes with the same

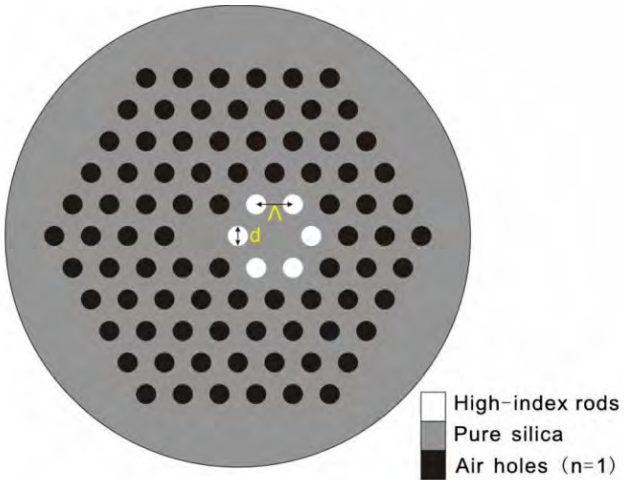

FIGURE 7. Cross section of the hybrid light-guiding wavelength-selective PCF coupler. (Reproduced with permission. [38] Copyright 2007, OSA).

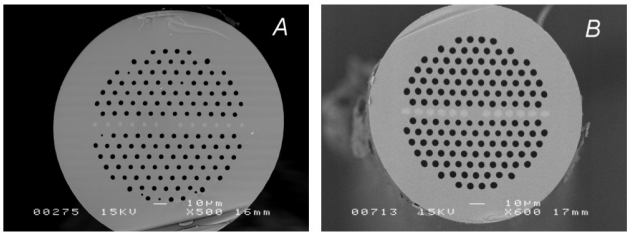

FIGURE 8. SEM images of fabricated hybrid photonic crystal fibers: (a) Δn= 1.0%, d= 3.2 μm, D=4.3 μm, and Λ =9.12 μm (d/Λ =0.35), (b) Δn=2.03%, d=3.88 μm, D=5.70 μm and Λ =7.15 μm (d/Λ =0.54). (Reproduced with permission. [15] Copyright 2006, OSA).

propagation constant and the couplings occur over a narrow spectral range, enabling promising applications in narrow band filtering applications [38]. Similar structures have been reported by infiltrating high refractive index liquid crystals into the air holes surround one of the silica core in a two-core PCF structure [39], [40].

Other guiding mechanisms, such as inhibited coupling-guiding mechanism, antiresonance-guiding mechanism, and twist-induce guiding mechanism can be realized in other types of PCF structures. They are explained in detail in [7] and are not discussed in this article.

III. REVIEW ON DEVELOPMENT AND APPLICATIONS OF HYBRID GUIDING PCFs

A. BACKGROUND

The first hybrid guiding PCF was fabricated using stack-and-draw technique. A standard multimode fiber preform with a plain silica cladding and a Ge-doped core was stacked with hollow silica capillaries and a single plain silica rod to form the bandgap guiding structure, whereas the index-guiding structure was formed by stacking silica capillaries in hexagonal pattern [15]. Two types of multimode preforms were used to fabricate the hybrid guiding PCFs, as shown in **Fig. 8**. Both fibers exhibited hybrid guiding mechanisms.

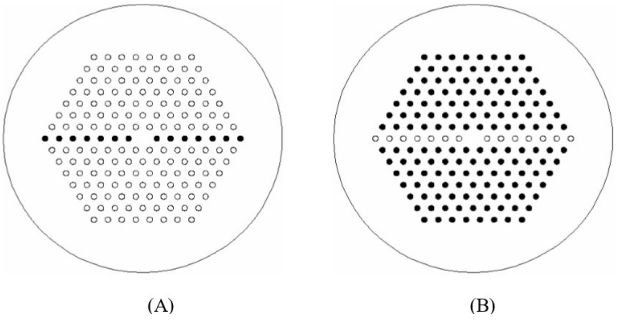

FIGURE 9. Schematics of cross-sections of two kinds of hybrid PCFs, whereas black holes are high index rods, empty holes are air holes. (Reproduced with permission. [16] Copyright 2007, OSA).

Subsequently, Xiao *et al.* presented an in-depth theoretical investigation of two kinds of hybrid guiding PCF structures using the same approach [16]. The schematics of two proposed hybrid guiding PCFs are shown in **Fig. 9**. There are several features observed in the modal analysis of the proposed hybrid guiding PCFs. Firstly, the fundamental modes are not degenerate due to the asymmetry of the transverse structure in two orthogonal directions. Secondly, the hybrid modes for light guiding only occur when both index-guiding and PBG-guiding are satisfied. As a result, the hybrid modes also exhibit discrete bands with cut-off wavelengths that are at the edges of the bandgap of the bandgap-guiding PCF. Thirdly, at the wavelength corresponding to the intersections of the dispersion curves of the index-guiding and bandgap-guiding PCF, the hybrid modes have the same mode index at the phase matching wavelength. In the analysis, index-guiding PCF refers to the structure without any high-index rods; whereas bandgap-guiding PCF refers to the structure in which all the air holes are replaced by the high-index rods.

Following the first experimental and theoretical reports on hybrid guiding PCFs [15], [16], the PCF research community has put significant efforts in understanding their properties, exploring and developing numerous hybrid guiding PCF-based applications such as tunable filters, high power lasers, nonlinear optics, and polarizations optics to various sensing applications. In subsequent sections, the reported applications are reviewed based on the approaches, namely polarization-dependent hybrid guiding PCFs, radial hybrid guiding PCFs and two-core hybrid guiding PCFs.

B. POLARIZATION-DEPENDENT HYBRID HUIDING PCFs

By breaking the mode degeneracy via utilizing the air holes and high index cladding structure along orthogonal directions, polarization-dependent guidance can be achieved in hybrid guiding PCFs. This approach has enabled several hybrid guiding PCF-based applications including lasers and amplifiers, single polarization operation and sensing which are reviewed in this section.

By introducing high index cladding structure along one transverse direction in the large mode area PCFs, the polarization-dependent hybrid guiding PCFs exhibit advantages of spectral filtering while maintaining single

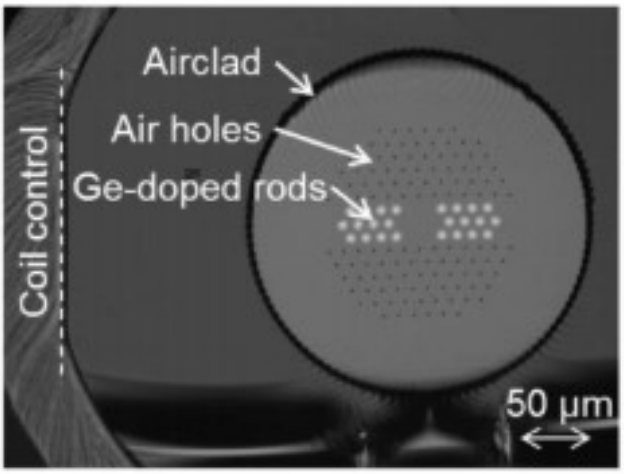

FIGURE 10. Microscopic image of the hybrid photonic crystal fiber. (Reproduced with permission. [41] Copyright 2015, OSA).

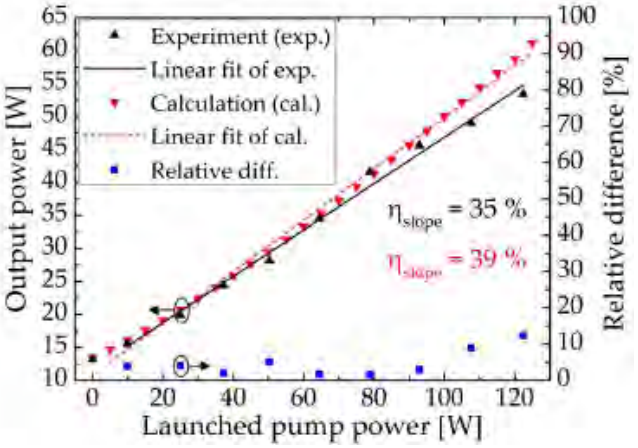

FIGURE 11. Measured and calculated output powers at 1178 *nm* as functions of launched pump powers for a seed power of 25 *W*. (Reproduced with permission. [41] Copyright 2015, OSA).

mode operation which are both desirable in lasers and amplifiers applications.

Yb^{3+}-doped fiber amplifier with hybrid guiding mechanisms that is used for amplification above 1100 nm was studied in recent years. Petersen *et al.* demonstrated a novel hybrid guiding Yb^{3+}-doped PCF amplifier with the fiber schematic as shown in **Fig. 10** [41]. The holey fiber cladding was modified by replacing three rows with high index inclusions to form bandgap guiding cladding for spectral filtering. The large core was formed by seven missing holes. The outer cladding is a ring of large air holes used for pump guidance. Compared with an earlier design having one row of high index inclusion [42], the proposed fiber achieved larger suppression of amplified spontaneous emission, improved gain shaping properties due to enhanced bandgap effect realized by more high index inclusions, and a larger modal birefringence due to the asymmetry [43].

Power scaling in the high power amplifiers requires special care in fiber design to address the limiting factors of nonlinear effects such as stimulated Raman scattering, stimulated Brillouin scattering, and four wave mixing (FWM). More importantly, it is necessary to remain single mode guidance with an increasing core size. The main advantages of using hybrid guiding PCFs in the power scaling applications are attributed to their abilties to maintain single mode operation and spectral filtering for suppressing undesirable nonlinear effects.

In the experimental study by Petersen *et al.* [41], a slope efficiency of 35% was obtained and an output power of 53*W* was achieved as shown in **Fig. 11**. Further power scaling was limited by parasitic lasing which was observed at 1000 *nm*.

Mart *et al.* presented an experimental study of using a hybrid microstructured Yb^{3+}-doped fiber amplifier, with large core diameter of 35 μm and spectral filtering for suppressing stimulated Brillouin scattering and modal instability. In addition, the feasibility of power scaling was also demonstrated by the hybrid microstructured fiber amplifier [44].

The FWM effects in large mode area (LMA) hybrid guiding PCFs were studied both theoretically and experimentally, showing that the LMA hybrid guiding PCFs can be used as effective waveguides to control and optimize the spectral position of the FWM products, thus providing more flexibility in developing high power amplifiers at wavelengths not easily accessible with e.g. rare earth ions [45]. Intermodal FWM process was demonstrated in hybrid guiding PCFs. Both co- and orthogonally polarized pump, signal and idler were used in the simulation for calculating the parametric gain. Intramodal birefringence assisted phase matching and intermodal phase matching were observed [46]. By controlling the polarization of the pump state between the principle axes of the LMA hybrid guiding PCF, the parametric gain of FWM can be switched on or off [47].

Besides using holey structure PCFs, hybrid guiding has also been reported using all solid PCFs, in which the core is pure silica and the low index F-doped silica rods array are arranged in hexagonal array in the cladding to form the index guidance, whereas the high-index Ge-doped silica rods are placed periodically along x-direction to form the bandgap guidance. The fiber schematic is shown in **Fig. 12** [48]. The proposed hybrid guiding fiber has enabled polarization maintaining operation in a fundamental mode which is spectrally filtered by photonic bandgap effect. Subsequently, a narrow linewidth Yb^{3+}-doped hybrid guiding PCF laser at 1178 *nm* was reported to demonstrate ASE suppression by the bandgap effect. The laser generated a narrow-linewidth (0.05 *nm*), 0.5 *W* CW output with 14% slope efficiency without the onset of parasitic lasing [49].

The polarization properties of the hybrid guiding PCFs have been exploited for single polarization guidance which is desirable for creating high polarization extinction ratio of linearly polarized fiber lasers and amplifiers [50], [51]. Goto *et al.* reported a birefringent hybrid microstructured fiber with extra B-doped SAPs for single polarization operation over 25 nm. The cross section of the fiber is shown in **Fig. 13** [50]. Another hybrid guiding PCF structure was report

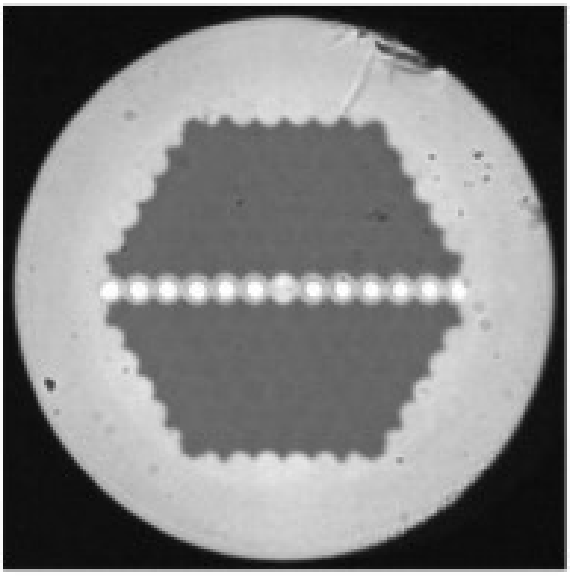

FIGURE 12. Cross section of the hybrid microstructured fiber. (Reproduced with permission. [48] Copyright 2008, OSA).

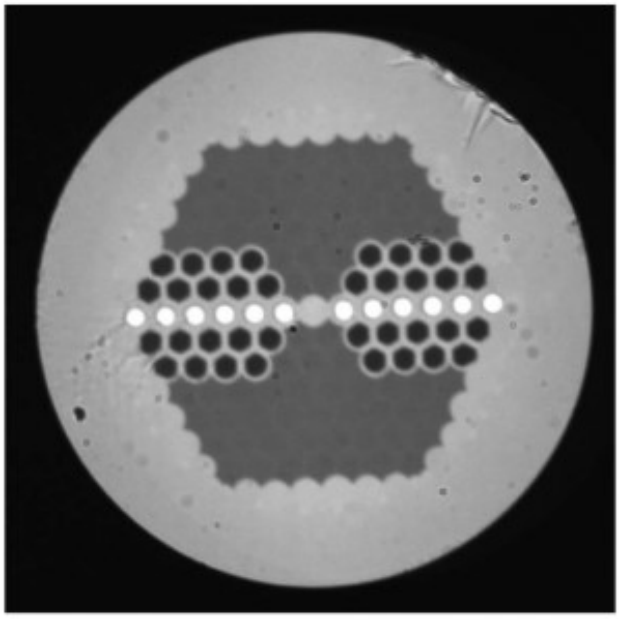

FIGURE 13. Cross section of fiber. (Reproduced with permission. [50] Copyright 2009, OSA).

for broadband single polarization operation over 225 nm [51]. The SEM of the hybrid PCF and the transmission spectra are shown in **Fig. 14**. The proposed structure has potential to develop multi- and broadband optical polarizers [52]. Polarized Bragg reflection was produced by a UV-induced Bragg grating in a single-polarization all-solid hybrid microstructured optical fiber, enabling the integration of polarizer and Bragg reflector within the same fiber which is desirable in constructing linearly polarized fiber lasers [53].

Hybrid guiding PCFs are used as sensing elements physical magnitudes by measuring the changes in transmission spectrum of the hybrid PCF sensor in interferometric

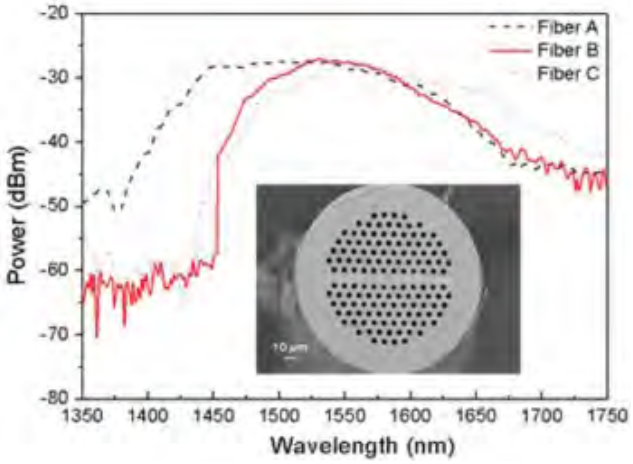

FIGURE 14. Transmission spectra of second PBGs. Inset, SEM of hybrid PCF. (Reproduced with permission. [51] Copyright 2011, OSA).

configurations. For example, Gu *et al.* used a modal interferometer configuration to detect strain and temperature and reported high strain sensitivity of 23.8 $pm/\mu\varepsilon$ and high temperature sensitivity of -1.12 $nm/^{\circ}C$ [54]. Birefringence resulted from the asymmetry of the structure in the hybrid guiding PCFs was measured against the temperature and strain using interferometric configurations [55]–[57]. Pang *et al.* studied the hybrid PCF sensor response to axial strain and temperature using Sagnac interferometry configuration, showing sensitivities of 2.01 $nm/m\varepsilon$ and -0.334 $nm/^{o}C$, respectively when the fringe measurement was monitored at the wavelength of 1550 *nm* [55]. A hybrid PCF strain sensor using cascaded Sagnac Interferometer configuration was reported to compensate temperature crosstalk. The experimental setup is shown in **Fig. 15**. The proposed sensor offered high strain sensitivity of 25.6 $pm/\mu\varepsilon$ and a low temperature sensitivity of -9 $pm/^{\circ}C$ [56]. By selectively infiltrating air holes of PCFs with tunable liquids, the birefringence of the hybrid PCF is controllable for sensing applications. Han et al. demonstrated that if the infiltrated liquids have higher index than that of silica, the coupled high-index-rod modes have impacts on the birefringence properties thus enabling sensing capability. Two hybrid PCFs (HPCFs) were used to construct temperature sensors, with temperature sensitivity of -45.8 $nm/^{\circ}C$ at $56.5^{\circ}C$ using one HPCF, and a sensitivity of -11.6 $nm/^{\circ}C$ from 65 $^{\circ}C$ to 85 $^{\circ}C$ was achieved using the other HPCF [57].

The experimental or theoretical investigation results of the polarization-dependent hybrid guiding PCFs-based devices are summarized in Table 1, for applications including lasers and amplifiers, single polarization operation and polarizers, and sensors.

C. RADIAL HYBRID GUIDING PCFs FOR FREQUENCY CONVERSION

Frequency conversion using all fiber devices in desirable wavelength regions is highly challenging and attractive for nonlinear optics applications. The generation of new

TABLE 1. Summary of polarization-dependent hybrid guiding PCFs and their applications.

Lasers and amplifiers

PCF structure	Signal wavelength(*nm*)	Output Power (*W*)	Slope efficiency	Reference
Holey Yb^{3+}-doped PCF with three rows of high index inclusion	1178	53	35%	Petersen et al. 2012 [43] & 2015 [41]
Holey Yb^{3+}-doped PCF with one row of high index inclusion	1064	9	>65%	Alkeskjold 2009 [42]
Holey Yb^{3+}-doped PCF with annularly gain tailored core, and three rows of high index inclusion	1064	820	78%	Mart et al. 2017 [44]
Holey Yb^{3+}-doped PCF with one row of high index inclusion for four-wave mixing (FWM)	848	1.2	17.3%	Petersen et al. 2013 [45] & 2015 [46]
Holey Yb^{3+}-doped PCF with one row of high index inclusion for polarization switch of four-wave mixing (FWM)	996	-50 *dBm*	-	Petersen et al. 2015 [47]
All solid bandgap PCF with one row of high index inclusion	1178	0.5	14%	Goto et al. 2008 [48] & 2009 [49]

Single Polarization (SP) and polarizers

PCF structure	SP Bandwidth (*nm*)	Polarization dependent loss (*dB*)	Reference
Birefringent hybrid microstructured fiber with extra B-doped SAP	25	-	Goto et al. 2009 [50]
Holey PCF with one row of high index inclusion	225	26.7	Cerqueira et al. 2011 [51] & 2012 [52]
All solid PCF with one row of high index inclusion and UV-induced Bragg grating	30	20	Goto et al. 2011 [53]

Sensors

PCF structure	Sensor configuration	Strain sensitivity ($pm/\mu\varepsilon$)	Temperature sensitivity ($nm/°C$)	Reference
All solid birefringent PCF	Modal interferometer	23.8	-1.12	Gu et al. 2011 [54]
Holey PCF with one row of high index inclusion	Sagnac interferometer	2.01	-0.334	Pang et al. 2012 [55]
All solid birefringent PCF	Cascaded Sagnac interferometer	25.6	-9×10^{-3}	Gu et al. 2012 [56]
Holey PCF with selective infiltration of high index liquid	Sagnac interferometer	-	-45.8	Han et al. 2014 [57]

frequencies from frequency conversion paves the way for extending the spectral range of laser resources for various applications. The challenges are mainly associated with the manipulation of the nonlinear effects and the dispersive effects, such as difficulties in fulfilling the phase matching conditions for harmonic generations. Radial hybrid guiding PCFs have been proposed and demonstrated as a suitable candidate for frequency conversion due to their flexibility in controlling the dispersion and nonlinearity.

Index guidance can be introduced into bandgap guiding PCFs by creating index difference between the core and the cladding, either by raising the refractive index of the core or lowering the effective index of the cladding. The first report of radial hybrid guiding PCF was proposed by Perrin *et al.* [31], and subsequently the structure was propsed for frequency doubling or tripling by Bétourné *et al.* [32]. The coexistence of both index-guiding and bandgap-guiding mechanism was demonstrated in the proposed structure illustrated in **Fig. 5(a)**. The introduction of interstitial air holes in photonic crystal cladding enabled the flexibility to lower the fundamental space filling mode index below the silica core index, thus making the index-guiding in the core possible with the defect core design by removing the first ring of the six interstitial air holes around the silica core. The phase matching for second and third harmonic generation using the proposed design were demonstrated theoretically, by adjusting the structural parameters such as the pitch, air hole size. In addition, the phase matching condition can be tuned

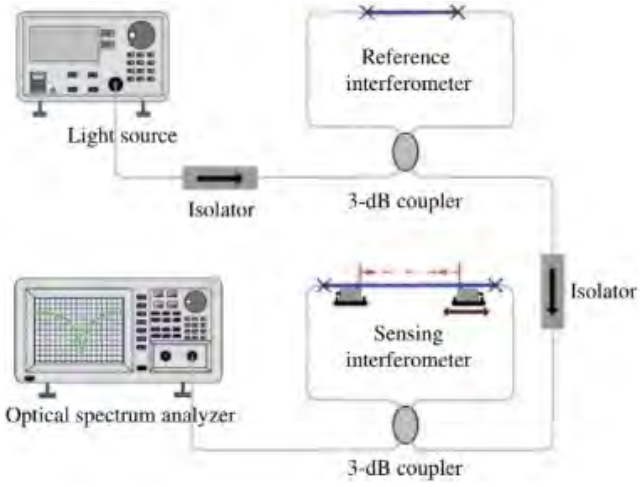

FIGURE 15. Schematic of the proposed cascaded Sagnac interferometers. (Reproduced with permission. [56] Copyright 2012, IEEE).

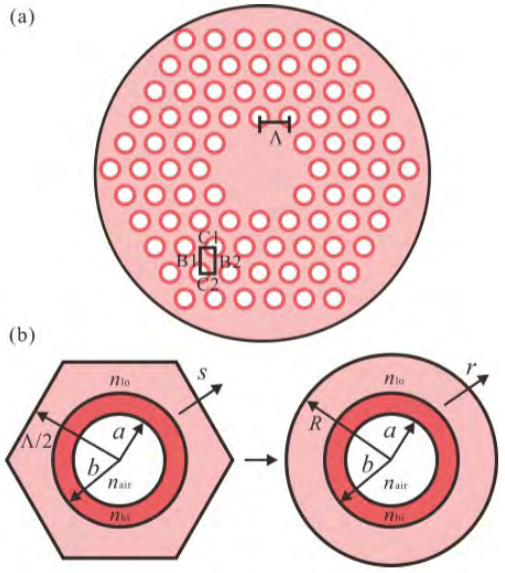

FIGURE 16. (a) Schematic of the PCF under study. HIRs (red, GGSS glass with RI = nhi) with IAHs (white, RI = nair) are arranged in a triangular lattice of pitch Λ in a low-index background (pink, TZLB glass with RI = nlo). The elementary cell B1C1B2C2 is used in the numerical method to compute the effective index of the cladding (also the top edge of the LP01 band). Seven HIR units are removed to form a multi-mode PCF. (b) A hexagonal unit cell on the left is approximated as a circular one on the right with the same are. a and b are, respectively, the inner and outer radii of the HIR. s is the local coordinate normal to the cell boundary while r is the radial coordinate in cylindrical coordinates. (Reproduced with permission. [33] Copyright 2016, IEEE).

spectrally by changing the structural parameters as well, which is desirable for harmonic generation [32]. Similar concept of achieving hybrid guiding mechanisms in PCF was reported by Lin *et al.*, using PCFs with a cladding of high-index arrays with internal air holes [33]. The proposed structure is shown in **Fig. 16**. The bandgap guidance was resulted from the periodic structure of high index rings (HIRs) in the cladding which are formed in a triangular lattice. The core was formed by 7 missing unit cells. The index guidance was achieved by lowering the effective index of the cladding

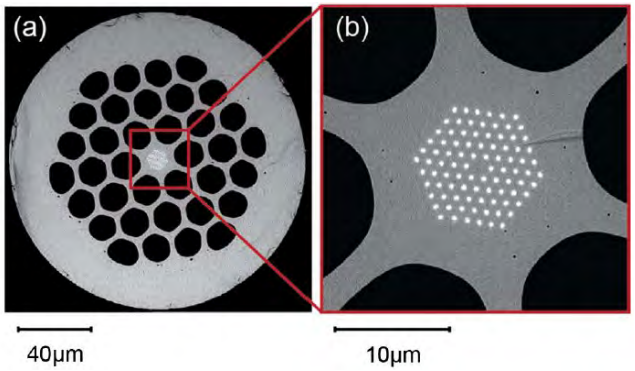

FIGURE 17. (a) Scanning electron micrograph of the hybrid fiber and (b) zooming into the all-solid bandgap microstructure. Black is air, gray is low-refractive-index glass (Schott LLF1), and white is high-refractive-index glass (Schott SF6). (Reproduced with permission. [37] Copyright 2016, OSA).

than that of the silica core. The proposed structure was simulated for coexistence of both guiding mechanisms associated with two guidance regions, i.e. 580-950 *nm* based on photonic bandgap effect and 2.0-4.6 μm based on index guiding mechanism respectively. In addition, the multi-modes were observed in both guidance regions which would facilitate the intermodal frequency conversion within each region or across the two guidance regions [33]. All solid PCFs (ASPCFs) were also demonstrated to achieve third order harmonic generation by phase matching the index-guided fundamental HE_{11} mode for the infrared source and a bandgap-guided higher-order HE_{12} mode for the ultraviolet radiation. The index guidance was achieved by raising the refractive index of the core than the effective index of the cladding [34].

For index guiding PCFs, bandgap guidance can be realized by creating a photonic crystal structure in the core region to achieve bandgap guided core modes, such as index-guiding PCF structure with a ring of high index rods around the silica core [35], [36] or with a hexagonal arrays of high index rods surrounding the core with lower index [37]. As illustrated in **Fig. 6**, the proposed design was demonstrated to have a bandgap-like core mode which has a broad spectral range and low confinement loss compared to all solid bandgap fiber. In addition, the index-guided core mode exist in long wavelengths. The features are desirable for mode filtering applications and nonlinear optics applications with appropriate phase matching conditions [35]. The same hybrid guiding fiber design was used to demonstrate the robustness of four-wave mixing stability [36].

More recently, Cavanna *et al.* reported a hybrid guiding PCF for third harmonic generation from 1596 nm to 532 *nm* in single-lobed modes [37]. The PCF structure is presented in **Fig. 17**, showing an all-solid PBG-PCF to guide the short wavelength signal, whereas the long wavelength signal is guided by index guidance resulted from the radial holey cladding. The index-guided fundamental mode is phase matched to the PBG-guided mode at third harmonic wavelength as shown in **Fig. 18**. Experimental investigations of the third harmonic generation were carried out using the

TABLE 2. Summary of radial hybrid guiding PCFs for frequency conversion.

PCF structure	Features	Reference
All solid PCF with interstitial air holes between the cladding rods	The fundamental wavelength for phase matching is tunable between 600 to 2000 *nm* by modifying the structure; Frequency doubling or tripling.	Bétourné et al. 2008 [32]
Chalcogenide–tellurite photonic crystal fiber (PCF) whose cladding is composed of a high-index array with internal regions being air	Guidance of 580-950 nm based on photonic bandgap effect and 2.0-4.6 μm based on index guiding mechanism; Multimode in both guidance range; Have potential of intermodal frequency conversion within each guidance region or across the two guidance regions.	Lin et al. 2016 [33]
All solid PCF with the doped core region	Third harmonic generation in the ultraviolet range, with fundamental wavelength of 1.06 μm	Bai et al. 2012 [34]
Holey PCF with higher refractive index inclusions in the first ring around the core	Broadband bandgap guidance and mode filtering	Ould-Agha et al. 2012 [35]
Holey PCF with higher refractive index inclusions in the first ring around the core	A phase-matched four wave mixing condition is demonstrated to be insensitive to scale fluctuations along the fiber length	Sévigny et al. 2013 [36]
Holey PCF with all-solid bandgap microstructure in the core region	Third harmonic generation from 1596 to 532 *nm* in single-lobed modes.	Cavanna et al. 2016 [37]

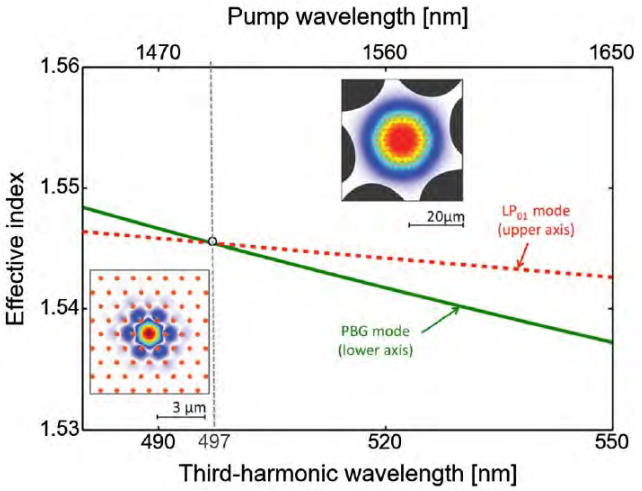

FIGURE 18. Refractive indices as a function of wavelength for the pump and the third harmonic modes, calculated by FEM using the dimensions of the fabricated fiber. The phase matching wavelengths are marked with a small circle. The upper inset shows the calculated Poynting vector distributions of the fundamental (LP01) mode at 1491 nm. The lower inset shows the third harmonic (PBG) mode at 497 nm. (Reproduced with permission. [37] Copyright 2016, OSA).

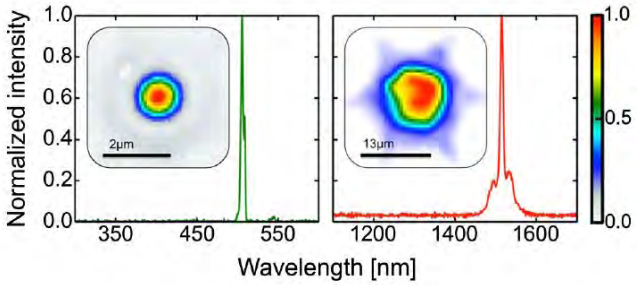

FIGURE 19. Spectrum of (a) the third harmonic and (b) the pump and the measured near-field intensity distributions of the corresponding modes. (Reproduced with permission. [37] Copyright 2016, OSA).

fabricated PCF that was pumped by an optical parametric generator and seeded with a tunable single frequency laser. The results are shown in **Fig. 19**, presenting the spectra of the pump signal and the third harmonic signal, as well as the measured near-field intensity of the corresponding modes. The results also confirmed a significant enhancement in the modal overlap for third harmonic generation in the fabricated PCF compared with standard step index fiber, showing promise to generate entangled photon triplets [37].

The investigations of radial hybrid guiding PCFs-for frequency conversion are summarized in **Table 2**.

D. TWO-CORE HYBRID GUIDING PCFs for FILTERING AND SENSING APPLICATIONS

Hybrid guiding PCFs with two-core structures have been reported for filtering and sensing applications. Such devices present significant phase mismatch between core modes by different guiding mechanisms, except at phase match wavelength. Therefore, it is possible to achieve several desirable features such as precise control of the filtering wavelength, narrow bandwidth of the coupling, side-lobe free coupling, and high sensitivity for sensing applications *etc*.

The first report of using two-core hybrid guiding PCFs for filtering application was presented by Sun [38]. The proposed

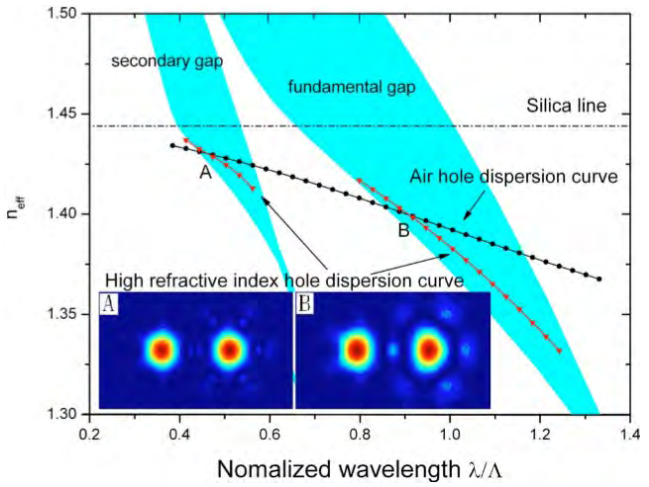

FIGURE 20. Modal dispersion curves for the fundamental mode of the single-core index-guiding PCF and single-core PBGF. The gray zones represent the fundamental gap and the secondary gap. The axes are effective index n_{eff} and normalized wavelength λ/Λ ; the curve with circles is the fundamental mode effective index computed for a simple index-guiding PCF formed by a pure silica core surrounded by holey silica. The curve with triangles shows the effective index of the high-index rods PBGF. The inset shows the intensity contour map at the intersect points A, $\lambda_0 = 1.55\mu m$ and B, $\lambda_0 = 3.21\mu m$, that is x-polarization electric field distribution mode (Ex). (Reproduced with permission. [38] Copyright 2007, OSA).

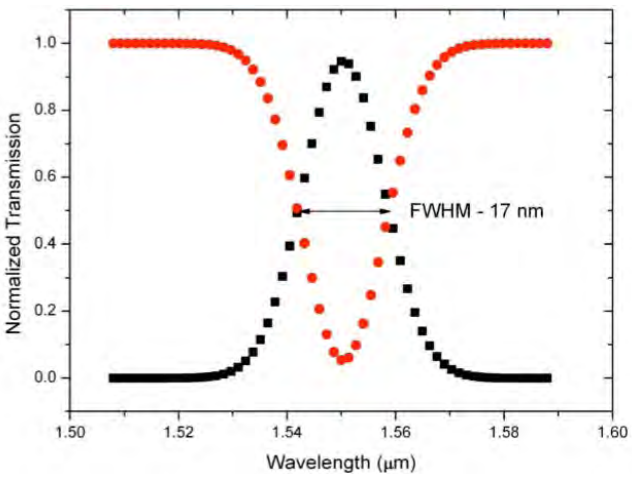

FIGURE 21. Spectral coupling characteristics of the hybrid light-guiding PCF coupler when we change the high-index middle hole between the two solid cores to air. The FWHM bandwidth is 17 nm and the used fiber length is 3.6 mm. (Reproduced with permission. [38] Copyright 2007, OSA).

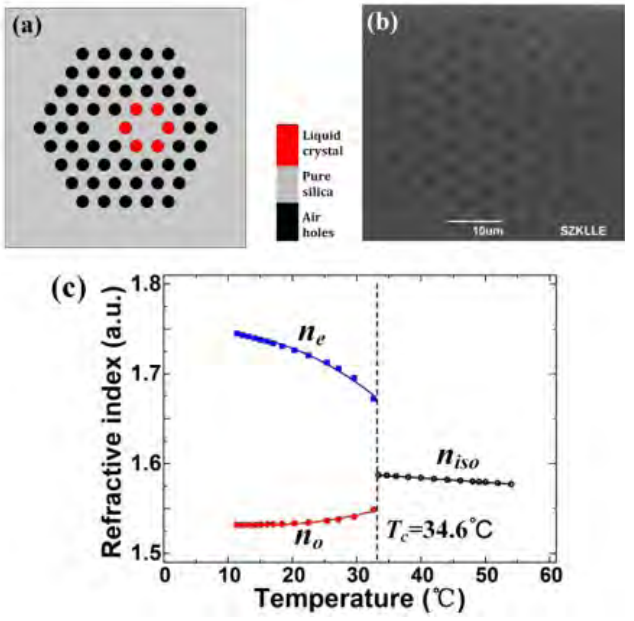

FIGURE 22. (a) Schematic diagram of the designed hybrid PCF; (b) SEM picture of the TCPCF used in this work; (c) Temperature dependence of RI of 5CB at wavelength of 589nm. (Reproduced with permission. [59] Copyright 2018, IOP).

fiber structure is shown in **Fig. 7**, in which two cores guide light based on index-guiding and PBG-guiding mechanism respectively. By treating each core as an individual waveguide, i.e. a single-core index-guiding PCF and a single-core photonic bandgap fiber (PBGF), the dispersion relationships and the phase matching wavelengths of the hybrid guiding PCF structure were analyzed for simplicity, as depicted in **Fig. 20**. The phase matching wavelengths between the two waveguides in the fundamental and the second bandgap of the PBG-guiding core are found at the intersections of the effective mode indices of the two core modes. The inset figures illustrate the mode profiles at the phase matching wavelengths in the hybrid PCF structure, showing overlaps of modal intensities between two cores. Complete power transfer between two cores occur at the coupling length of the hybrid PCF structure, which is significantly shorter than conventional optical fiber couplers. Furthermore, the proposed structure can be optimized by replacing the central high-index rod to a void for narrowband power coupling between two cores as presented in **Fig. 21**, which enables the narrowband filtering applications at desirable wavelengths. The computed coupling bandwidth is 17 *nm* using a 3.6 *mm* hybrid guiding PCF structure with a void in the center between two cores.

By introducing thermally tunable materials into the hybrid guiding PCF structures, such as high refractive index liquid crystals to create photonic bandgap structure, Hu *et al.* reported and demonstrated thermal tunability of a hybrid guiding PCF coupler with promising potential for filtering and sensing applications [39].

By monitoring the spectra properties such as the resonance wavelengths and/or the intensity, hybrid guiding PCFs were proposed and demonstrated for highly sensitive sensing measurements in recent years [40, 58, 59]. Xu *et al.* used a twin core PCF structure with selective infiltration of high refractive index liquid crystal, 5CB into the air holes around one of the solid core to realize the coexistence of bandgap guiding mechanism and the index guiding mechanism. The PCF structure and the refractive index profile of the liquid crystal used in the work is shown in **Fig. 22**. Due to the thermal tunability of the refractive index of the liquid crystal, the proposed structure was experimentally demonstrated to exhibit high temperature sensitivity of up to 4.91 *nm/°C* for nematic phase of 5CB, and -3.68 *nm/°C* for isotropic phase of 5CB as shown in Figure 23, respectively, which could find

TABLE 3. Summary of two-core hybrid guiding PCFs for filtering and sensing applications.

PCF structure	Application and Features	Reference
Holey two-core PCF, with one core surrounded by one ring of high index inclusion	Wavelength-selective coupling for filtering and sensing applications; the full-width half-maximum of the coupling bandwidth is 17 nm in an optimized design;	Sun 2007 [38]
Holey two-core PCF, with one core surrounded by three rings of high index inclusion	Thermally tunable coupler; the phase matching wavelength shifts from 1.52 to 1.62 μm as temperature varies from 30 to 50 $^{\circ}C$	Hu et al. 2009 [39]
Holey two-core PCF, with one core surrounded by one ring of high index inclusion	Temperature sensor; 4.91 $nm/^{\circ}C$ for nematic phase of 5CB, and -3.68 $nm/^{\circ}C$ for isotropic phase of 5CB	Hu et al. 2017 [40] Xu et al. 2018 [58] [59]

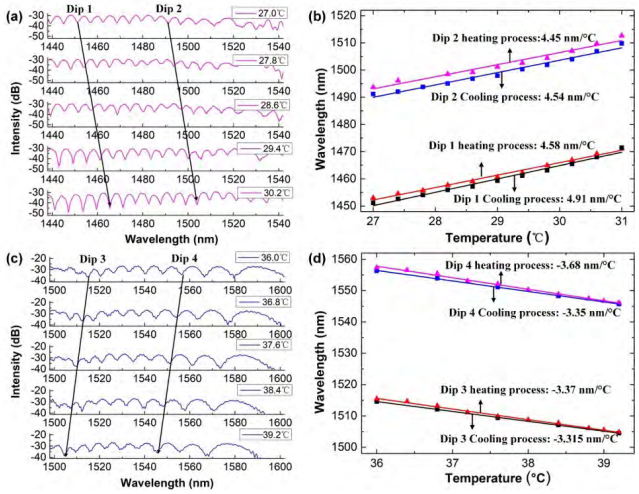

FIGURE 23. Experimental results for temperature response of the hybrid PCF. (a) and (b) are results for temperature below the clearing temperature: (a) Transmission spectra of the hybrid PCF under different temperature; (b) dependence of resonant wavelengths of Dip 1 and Dip 2 on the temperature. (c) and (d) are results for temperature higher than the clearing temperature: (c) Transmission spectra of the hybrid PCF under different temperature; (d) dependence of resonant wavelengths of Dip 3 and Dip 4 on the temperature. (Reproduced with permission. [59] Copyright 2018, IOP).

applications in temperature-tunable optical filtering in optical fiber communication, sensing and laser systems.

The results of two-core hybrid guiding PCFs-for filtering and sensing applications are summarized in **Table 3.**

IV. CONCLUSION and PERSPECTIVES

The co-existence of index-guiding and bandgap-guiding mechanism in the hybrid guiding PCFs has provided great flexibility in shaping and controlling the light propagation properties, thus enabling versatile functionalities and applications to be achieved. There has been significant development and growth in the hybrid guiding PCF technology recently. The three major approaches to construct the hybrid guiding PCFs are reviewed thoroughly in the paper, from the perspectives of both the technology and applications. Hybrid guiding PCFs can be modified from the structures of both index-guiding PCFs and bandgap-guiding PCFs by introducing the structure that relies on the other guiding mechanism into the fiber. The bandgap-guiding structure can be realized by arrays of high-index inclusions such as Ge-doped rods or high-index fluids that are introduced into one direction of the waveguide cross section. The index-guiding structure can be based on holey structure or arrays of low-index inclusions such as F-doped rods. Polarization-dependent hybrid guiding PCFs possess index-guiding and bandgap-guiding mechanism in the orthogonal directions respectively by breaking the symmetry in the waveguide structure. They are developed for applications in lasers and amplifiers, single polarization operation and sensing for various parameters. Radial hybrid guiding PCFs retain the structure symmetry, but differ in guiding mechanisms in the inner and outer structure. They are demonstrated as a suitable structure for fiber based frequency conversion which is promising to develop all fiber based nonlinear optic devices and applications. Two-core hybrid guiding PCFs possess different guiding mechanisms in each core, exhibiting properties of precise control of the filtering wavelength, narrow bandwidth of the coupling and side-lobe free coupling. Two-core hybrid guiding PCFs have been reported for high sensitivity for sensing applications.

The precise control of mode coupling between the index-guiding and bandgap-guiding modes is critical to ensure the performance of the designed structure and device. It is noted that the challenges of developing hybrid PCF based devices and applications are mainly due to the technical challenges in fabricating the intricate features of the PCF structures with good uniformity along fiber length. Therefore, the rapid progress in PCF fabrication technologies and post-processing techniques are favorable to develop hybrid guiding PCF devices in ensuring the precision of microstructures in the fiber, thus minimizing the discrepancies between the design and the actual performance. Hybrid guiding PCFs are expected to provide more opportunities in developing scientific and industrial applications.

REFERENCES

[1] P. Russell, "Photonic crystal fibers," *Science*, vol. 299, no. 5605, pp. 358–362, 2003.
[2] J. C. Knight, "Photonic crystal fibres," *Nature*, vol. 424, pp. 847–851, Aug. 2003.
[3] P. S. J. Russell, "Photonic-crystal fibers," *J. Lightw. Technol.*, vol. 24, no. 12, pp. 4729–4749, Jul. 2006.

[4] A. M. R. Pinto and M. Lopez-Amo, "Photonic crystal fibers for sensing applications," *J. Sensor*, vol. 2012, Feb. 2012, Art. no. 598178.
[5] J. Villatoro and J. Zubia, "New perspectives in photonic crystal fibre sensors," *Opt. Laser Technol.*, vol. 78, pp. 67–75, Apr. 2016.
[6] D. J. J. Hu, R. Y.-N. Wong, and P. P. Shum, "Photonic crystal fiber-based interferometric sensors," in *Selected Topics on Optical Fiber Technologies and Applications*. Rijeka, Croatia: InTech, 2018, pp. 21–41.
[7] C. Markos, J. C. Travers, A. Abdolvand, B. J. Eggleton, and O. Bang, "Hybrid photonic-crystal fiber," *Rev. Mod. Phys.*, vol. 89, no. 4, 2017, Art. no. 045003.
[8] S. Ertman, P. Lesiak, and T. R. Woliński, "Optofluidic photonic crystal fiber-based sensors," *J. Lightw. Technol.*, vol. 35, no. 16, pp. 3399–3405, Aug. 15, 2017.
[9] X. Yang, C. Shi, R. Newhouse, J. Z. Zhang, and C. Gu, "Hollow-core photonic crystal fibers for surface-enhanced Raman scattering probes," *Int. J. Opt.*, vol. 2011, Feb. 2011, Art. no. 754610.
[10] Y. Zhao, Z.-Q. Deng, and J. Li, "Photonic crystal fiber based surface plasmon resonance chemical sensors," *Sens. Actuators B, Chem.*, vol. 202, pp. 557–567, Oct. 2014.
[11] D. J. J. Hu and H. P. Ho, "Recent advances in plasmonic photonic crystal fibers: Design, fabrication and applications," *Adv. Opt. Photon.*, vol. 9, no. 2, pp. 257–314, 2017.
[12] J. C. Knight, "Photonic crystal fibers and fiber lasers," *J. Opt. Soc. Amer. B, Opt. Phys.*, vol. 24, no. 8, pp. 1661–1668, 2007.
[13] J. C. Knight and D. V. Skryabin, "Nonlinear waveguide optics and photonic crystal fibers," *Opt. Express*, vol. 15, no. 23, pp. 15365–15376, 2007.
[14] J. C. Travers, W. Chang, J. Nold, N. Y. Joly, and P. S. J. Russell, "Ultrafast nonlinear optics in gas-filled hollow-core photonic crystal fibers," *J. Opt. Soc. Amer. B, Opt. Phys.*, vol. 28, no. 12, pp. A11–A26, 2011.
[15] S. A. Cerqueira, Jr., F. Luan, C. M. B. Cordeiro, A. K. George, and J. C. Knight, "Hybrid photonic crystal fiber," *Opt. Express*, vol. 14, no. 2, pp. 926–931, 2006.
[16] L. Xiao, W. Jin, and M. S. Demokan, "Photonic crystal fibers confining light by both index-guiding and bandgap-guiding: Hybrid PCFs," *Opt. Express*, vol. 15, no. 24, pp. 15637–15647, 2007.
[17] T. A. Birks, J. C. Knight, and P. S. J. Russell, "Endlessly single-mode photonic crystal fiber," *Opt. Lett.*, vol. 22, no. 13, pp. 961–963, Jul. 1997.
[18] N. A. Issa, "High numerical aperture in multimode microstructured optical fibers," *Appl. Opt.*, vol. 43, no. 33, pp. 6191–6197, 2004.
[19] M. Napierała, T. Nasilowski, E. Bereś-Pawlik, P. Mergo, F. Berghmans, and H. Thienpont, "Large-mode-area photonic crystal fiber with double lattice constant structure and low bending loss," *Opt. Express*, vol. 19, no. 23, pp. 22628–22636, 2011.
[20] D. J. J. Hu, F. Luan, and P. P. Shum, "All-glass leakage channel fibers with triangular core for achieving large mode area and low bending loss," *Opt. Commun.*, vol. 284, no. 7, pp. 1811–1814, 2011.
[21] K. P. Hansen, "Dispersion flattened hybrid-core nonlinear photonic crystal fiber," *Opt. Express*, vol. 11, no. 13, pp. 1503–1509, 2003.
[22] D. J. J. Hu, P. P. Shum, C. Lu, and G. Ren, "Dispersion-flattened polarization-maintaining photonic crystal fiber for nonlinear applications," *Opt. Commun.*, vol. 282, no. 20, pp. 4072–4076, 2009.
[23] J. Ju, W. Jin, and M. S. Demokan, "Design of single-polarization single-mode photonic crystal fiber at 1.30 and 1.55 μm," *J. Lightw. Technol.*, vol. 24, no. 2, pp. 825–830, Feb. 2006.
[24] D. J. J. Hu, P. Shum, C. Lu, X. Yu, G. Wang, and G. Ren, "Holey fiber design for single-polarization single-mode guidance," *Appl. Opt.*, vol. 48, no. 20, pp. 4038–4043, 2009.
[25] A. Ortigosa-Blanch, J. C. Knight, W. J. Wadsworth, J. Arriaga, B. J. Mangan, T. A. Birks, and P. S. J. Russell, "Highly birefringent photonic crystal fibers," *Opt. Lett.*, vol. 25, no. 18, pp. 1325–1327, 2000.
[26] T. P. Hansen, J. Broeng, S. E. B. Libori, E. Knudsen, A. Bjarklev, J. R. Jensen, and H. Simonsen, "Highly birefringent index-guiding photonic crystal fibers," *IEEE Photon. Technol. Lett.*, vol. 13, no. 6, pp. 588–590, Jun. 2001.
[27] J. K. Lyngsø, B. J. Mangan, C. B. Olausson, and P. J. Roberts, "Stress induced birefringence in hybrid TIR/PBG guiding solid photonic crystal fibers," *Opt. Express*, vol. 18, no. 13, pp. 14031–14040, 2010.
[28] K. Milenko, T. R. Wolinski, D. J. J. Hu, J. L. Lim, Y. Wang, and P. P. Shum, "Hybrid photonic crystal fiber selectively infiltrated with liquid crystal," in *Proc. Photon. Global Conf.*, Singapore, Dec. 2012, pp. 1–3.
[29] J. Sun and C. C. Chan, "Hybrid guiding in liquid-crystal photonic crystal fibers," *J. Opt. Soc. Amer. B, Opt. Phys.*, vol. 24, no. 10, pp. 2640–2646, 2007.
[30] G. Ren, P. Shum, J. Hu, X. Yu, and Y. Gong, "Study of polarization-dependent bandgap formation in liquid crystal filled photonic crystal fibers," *IEEE Photon. Technol. Lett.*, vol. 20, no. 8, pp. 602–604, Apr. 15, 2008.
[31] M. Perrin, Y. Quiquempois, G. Bouwmans, and M. Douay, "Coexistence of total internal reflexion and bandgap modes in solid core photonic bandgap fibre with intersticial air holes," *Opt. Express*, vol. 15, no. 21, pp. 13783–13795, 2007.
[32] A. Bétourné, Y. Quiquempois, G. Bouwmans, and M. Douay, "Design of a photonic crystal fiber for phase-matched frequency doubling or tripling," *Opt. Express*, vol. 16, no. 18, pp. 14255–14262, 2008.
[33] P. Lin, Y. Li, T. Cheng, T. Suzuki, and Y. Ohishi, "Coexistence of photonic bandgap guidance and total internal reflection in photonic crystal fiber based on a high-index array with internal air holes," *IEEE J. Sel. Topics Quantum Electron.*, vol. 22, no. 2, Mar./Apr. 2016, Art. no. 4900606.
[34] J. Bai, W. Xing, C. Yang, Y. Li, and D. M. Bird, "Strategy to achieve phase matching condition for third harmonic generation in all-solid photonic crystal fibers," *IEEE Photon. Technol. Lett.*, vol. 24, no. 5, pp. 389–391, Mar. 2012.
[35] Y. Ould-Agha, A. Bétourné, O. Vanvincq, G. Bouwmans, and Y. Quiquempois, "Broadband bandgap guidance and mode filtering in radially hybrid photonic crystal fiber," *Opt. Express*, vol. 20, no. 6, pp. 6746–6760, 2012.
[36] B. Sévigny, O. Vanvincq, C. Valentin, N. Chen, Y. Quiquempois, and G. Bouwmans, "Four-wave mixing stability in hybrid photonic crystal fibers with two zero-dispersion wavelengths," *Opt. Express*, vol. 21, no. 25, pp. 30859–30873, 2013.
[37] A. Cavanna, F. Just, X. Jiang, G. Leuchs, M. V. Chekhova, P. S. J. Russell, and N. Y. Joly, "Hybrid photonic-crystal fiber for single-mode phase matched generation of third harmonic and photon triplets," *Optica*, vol. 3, no. 9, pp. 952–955, 2016.
[38] X. Sun, "Wavelength-selective coupling of dual-core photonic crystal fiber with a hybrid light-guiding mechanism," *Opt. Lett.*, vol. 32, no. 17, pp. 2484–2486, 2007.
[39] D. J. J. Hu, P. Shum, C. Lu, X. Sun, G. Ren, X. Yu, and G. Wang, "Design and analysis of thermally tunable liquid crystal filled hybrid photonic crystal fiber coupler," *Opt. Commun.*, vol. 282, no. 12, pp. 2343–2347, 2009.
[40] D. J. J. Hu, Z. Xu, S. Ertman, T. Wolinski, and W. Tong, "Two core photonic crystal fiber with hybrid guiding mechanisms," in *Proc. Conf. Lasers Electro-Opt. Pacific Rim (CLEO-PR)*, Singapore, Jul./Aug. 2017, pp. 1–3.
[41] S. R. Petersen, M. Chen, A. Shirakawa, C. B. Olausson, T. T. Alkeskjold, and J. Lægsgaard, "Large-mode-area hybrid photonic crystal fiber amplifier at 1178 nm," *Opt. Lett.*, vol. 40, no. 8, pp. 1741–1744, 2015.
[42] T. T. Alkeskjold, "Large-mode-area ytterbium-doped fiber amplifier with distributed narrow spectral filtering and reduced bend sensitivity," *Opt. Express*, vol. 17, no. 19, pp. 16394–16405, 2009.
[43] S. R. Petersen, T. T. Alkeskjold, F. Poli, E. Coscelli, M. M. Jørgensen, M. Laurila, J. Lægsgaard, and J. Broeng, "Hybrid Ytterbium-doped large-mode-area photonic crystal fiber amplifier for long wavelengths," *Opt. Express*, vol. 20, no. 6, pp. 6010–6020, 2012.
[44] C. Mart, B. Pulford, B. Ward, I. Dajani, T. Ehrenreich, B. Anderson, K. Kieu, and T. Sanchez, "Power scaling of a hybrid microstructured Yb-doped fiber amplifier," *Proc. SPIE*, vol. 10083, Feb. 2017, Art. no. 100830X.
[45] S. R. Petersen, T. T. Alkeskjold, and J. Lægsgaard, "Degenerate four wave mixing in large mode area hybrid photonic crystal fibers," *Opt. Express*, vol. 21, no. 15, pp. 18111–18124, 2013.
[46] S. R. Petersen, T. T. Alkeskjold, C. B. Olausson, and J. Lægsgaard, "Intermodal and cross-polarization four-wave mixing in large-core hybrid photonic crystal fibers," *Opt. Express*, vol. 23, no. 5, pp. 5954–5971, 2015.
[47] S. R. Petersen, T. T. Alkeskjold, C. B. Olausson, and J. Lægsgaard, "Polarization switch of four-wave mixing in large mode area hybrid photonic crystal fibers," *Opt. Lett.*, vol. 40, no. 4, pp. 487–490, 2015.
[48] R. Goto, S. D. Jackson, S. Fleming, B. T. Kuhlmey, B. J. Eggleton, and K. Himeno, "Birefringent all-solid hybrid microstructured fiber," *Opt. Express*, vol. 16, no. 23, pp. 18752–18763, 2008.
[49] R. Goto, E. C. Magi, and S. D. Jackson, "Narrow-linewidth, yb^{31}-doped, hybrid microstructured fibre laser operating at 1178 nm," *Electron. Lett.*, vol. 45, no. 17, pp. 877–878, Aug. 2009.
[50] R. Goto, S. D. Jackson, and K. Takenaga, "Single-polarization operation in birefringent all-solid hybrid microstructured fiber with additional stress applying parts," *Opt. Lett.*, vol. 34, no. 20, pp. 3119–3121, 2009.

[51] S. A. Cerqueira, Jr., D. G. Lona, I. de Oliveira, H. E. Hernandez-Figueroa, and H. L. Fragnito, "Broadband single-polarization guidance in hybrid photonic crystal fibers," *Opt. Lett.*, vol. 36, no. 2, pp. 133–135, 2011.
[52] S. A. Cerqueira, Jr., A. R. D. Nascimento, Jr., M. A. R. Franco, I. de Oliveira, V. A. Serrão, and H. L. Fragnito, "Numerical and experimental analysis of polarization properties from hybrid PCFs across different photonic bandgaps," *Opt. Fiber Technol.*, vol. 18, no. 6, pp. 462–469, 2012.
[53] R. Goto, I. Fsaifes, A. Baz, L. Bigot, K. Takenaga, S. Matsuo, and S. D. Jackson, "UV-induced Bragg grating inscription into single-polarization all-solid hybrid microstructured optical fiber," *Opt. Express*, vol. 19, no. 14, pp. 13525–13530, 2011.
[54] B. Gu, W. Yuan, A. P. Zhang, and O. Bang, "All-solid birefringent hybrid photonic crystal fiber based interferometric sensor for measurement of strain and temperature," in *Proc. Asia Commun. Photon. Conf. Exhib. (ACP)*, Shanghai, China, Nov. 2011, pp. 1–7.
[55] M. Pang, L. M. Xiao, W. Jin, and S. A. Cerqueira, Jr., "Birefringence of hybrid PCF and Its sensitivity to strain and temperature," *J. Lightw. Technol.*, vol. 30, no. 10, pp. 1422–1431, May 15, 2012.
[56] B. Gu, W. Yuan, S. He, and O. Bang, "Temperature compensated strain sensor based on cascaded Sagnac interferometers and all-solid birefringent hybrid photonic crystal fibers," *IEEE Sensors J.*, vol. 12, no. 6, pp. 1641–1646, Jun. 2012.
[57] T. Han, Y.-G. Liu, Z. Wang, J. Guo, Z. Wu, M. Luo, S. Li, J. Wang, and W. Wang, "Control and design of fiber birefringence characteristics based on selective-filled hybrid photonic crystal fibers," *Opt. Express*, vol. 22, no. 12, pp. 15002–15016, Jun. 2014.
[58] Z. Xu, D. J. J. Hu, Z. Wu, S. Ertman, T. Wolinski, W. Tong, and P. P. Shum, "Highly sensitive temperature sensor based on hybrid photonic crystal fiber," in *Proc. Opt. Fiber Commun. Conf.*, Mar. 2018, pp. 1–3, Paper W2A.13.
[59] Z. Xu, B. Li, D. J. J. Hu, Z. Wu, S. Ertman, T. Wolinski, W. Tong, and P. P. Shum, "Hybrid photonic crystal fiber for highly sensitive temperature measurement," *J. Opt.*, vol. 20, no. 7, 2018, Art. no. 075801.

DORA JUAN JUAN HU received the B.Eng. degree (Hons.) and Ph.D. degree from the School of Electrical and Electronic Engineering, Nanyang Technological University, Singapore, in 2004 and 2010, respectively. From 2009 to 2012, she was with the RF & Optical Department, Institute for Infocomm Research (I2R), Agency for Science, Technology, and Research (A*STAR), Singapore, as a Scientist and a Principle Investigator to develop novel fiber devices for sensor applications. In 2012, she received A*STAR Postdoctoral Fellowship (2012–2014). In 2012, she joined the Wellman Center for Photomedicine, Massachusetts General Hospital, Boston, MA, USA, as a Research Fellow and involved in novel photonic technologies for endoscopic diagnosis. She joined the Femtosecond Optics Group, Imperial College London, in 2013, where she was involved in visible and mid-infrared fiber lasers. She is currently with the Infrastructure, Energy and Environment Department, I2R, A*STAR, Singapore, as the Environment Unit Head, involved in novel photonic technologies for sensing and biomedical applications.

ZHILIN XU received the B.Sc. degree in optical information science and technology from Nanchang University, China, in 2011, and the Ph.D. degree in optical engineering from the Huazhong University of Science and Technology, China, in 2016. From 2016 to 2018, she was a Postdoctoral Research Fellow with the Centre for Optical Fiber Technology, Nanyang Technological University, Singapore. Since 2018, she has been an Associate Professor with the Center for Gravitational Experiments, Huazhong University of Science and Technology, Wuhan, China. Her research interests include optical fiber sensors, fiber optic microstructure devices, and optical precision measurement.

PERRY PING SHUM received the B.Eng. and Ph.D. degrees in electronic and electrical engineering from the University of Birmingham, U.K., in 1991 and 1995, respectively, where he was an Honorary Postdoctoral Research Fellow. In 1996, he carried out research in semiconductor laser and high speed optical laser communication with the Department of Electrical and Electronic Engineering, Hong Kong University. In 1997, he joined the Department of Electronic Engineering, Optoelectronics Research Centre, City University of Hong Kong. In 1999, he joined the School of Electrical and Electronic Engineering, Nanyang Technological University. He has published more than 300 international journal and conference papers. His research interests include optical communications, nonlinear waveguide modeling, fiber gratings, and WDM communication systems. In 1998, he has received the IEEE EDS/MTTS India Chapter Best Paper Award for his paper in Photonics-98. In 2002, he received the Best Paper Award from the 3rd International Conference on Microwave and Millimeter Wave Technology. He is also the Founding Member of the IEEE LEOS chapter, Singapore. In 2002, he was appointed as the Director of the Network Technology Research Centre. He received the Singapore National Academy of Science Young Scientist Award, in 2002. He is the Technical Program Chair of ICOCN 2003 and committee members and international advisor of many international conferences.